



**QUEEN'S  
UNIVERSITY  
BELFAST**

## High brightness laser induced multi-MeV electron/proton sources

Giulietti, D., Breschi, E., Galimberti, M., Borghesi, M., Giulietti, A., Gizzi, L. A., Koester, P., Labate, L., Tomassini, P., Ceccotti, T., De Olivera, P., Monot, P., Romagnani, L., Kar, S., Bertolucci, S., Calveti, M., Schiavi, A., & Willi, O. (2007). High brightness laser induced multi-MeV electron/proton sources. *International Journal of Modern Physics A*, 22(22), 3810-3817.

**Published in:**

International Journal of Modern Physics A

**Document Version:**

Publisher's PDF, also known as Version of record

**Queen's University Belfast - Research Portal:**

[Link to publication record in Queen's University Belfast Research Portal](#)

**General rights**

Copyright for the publications made accessible via the Queen's University Belfast Research Portal is retained by the author(s) and / or other copyright owners and it is a condition of accessing these publications that users recognise and abide by the legal requirements associated with these rights.

**Take down policy**

The Research Portal is Queen's institutional repository that provides access to Queen's research output. Every effort has been made to ensure that content in the Research Portal does not infringe any person's rights, or applicable UK laws. If you discover content in the Research Portal that you believe breaches copyright or violates any law, please contact [openaccess@qub.ac.uk](mailto:openaccess@qub.ac.uk).

## HIGH BRIGHTNESS LASER INDUCED MULTI-MEV ELECTRON/PROTON SOURCES\*

D. GIULIETTI<sup>†</sup>, E. BRESCHI, M. GALIMBERTI, A. GIULIETTI, L.A. GIZZI,  
P. KOESTER, L. LABATE, P. TOMASSINI

*Intense Laser Irradiation Laboratory, IPCF-CNR, Pisa and INFN-Pisa, Italy*

PH. MARTIN, T. CECCOTTI, P. DE OLIVERA, P. MONOT

*Physique à Haute Intensité, CEA-DSM/DRECAM/SPAM, Saclay, France*

M. BORGHESI, L. ROMAGNANI, S. KAR

*Queen's University of Belfast, UK*

S. BERTOLUCCI, M. CALVETTI

*Laboratori Nazionali di Frascati, INFN, Italy*

A. SCHIAVI

*Dipartimento di Energetica, Università "la Sapienza", Roma, Italy*

O. WILLI

*Heinrich-Heine Universität Dusseldorf, Germany*

The chirped pulse amplification (CPA) technique has opened new perspectives in the radiation-matter interaction studies using ultra-short laser pulses at ultra-relativistic intensities. In particular the original idea, proposed by Tajima and Dawson, of accelerating electrons by the huge electric fields of plasma waves which develop in the wake of a laser pulse propagating in a plasma, become feasible. Some laboratories all over the world have produced by such a technique collimated electron bunches of hundreds of MeV along acceleration lengths of a few hundreds of microns. In other experiments, using thin solid targets, intense bursts of energetic protons have been at the same time detected. The proton acceleration mechanism is essentially based on the Coulomb force appearing at the thin solid target surface as a consequence of the previous escape of the energetic electrons from the target. In the paper some experimental results will be presented as well as the opportunities the INFN PLASMONX project will offer in this research field at LNF.

---

\* This work is partially supported by INFN project PLASMONX.

<sup>†</sup> Also at Physics Department of Pisa University, Largo B. Pontecorvo n.3, 56127, Pisa, Italy.  
E-mail : danilo.giulietti@df.unipi.it

## 1. Introduction

The current slowing down of further development of the experimental research in high energy particle physics is mainly due to the gigantism of conventional particle accelerators and their cost hardly sustainable, even by international consortia as the CERN.

The size of conventional accelerators producing high energies particles have to be very large in both cases of linear and circular acceleration. In fact, the maximum allowed accelerating electric field must be below the material breakdown threshold which is typically of the order of several tens of MV/m. In the case of a 1TeV accelerator, this condition sets an acceleration length not less than 20Km for an accelerating field of 50MV/m. In the case of circular accelerators, relatively large dimensions are still required, because of the synchrotron radiation losses.

This breakdown limitation does not apply to plasmas which are therefore regarded as the ideal medium in which charged particles can be accelerated by means of electric fields that are order of magnitude higher than those of conventional accelerators [1]. After the first pioneering experiments on plasma accelerators carried out in the early eighties, impressive progress in this field is being achieved today, following the advent of the ultra-short pulse lasers and the Chirped Pulse Amplification (CPA) technique [2]. In fact, thanks to CPA, pulses of a few joules in tens of femtoseconds can now be produced and used to induce the huge electric fields that can accelerate charged particles up to 1GeV in a few mm length. In the last years theoretical and experimental activity has been developed achieving more and more encouraging results concerning the energy and the quality of the electron/proton beam produced by laser-driven acceleration mechanisms [3, 4, 5, 6, 7, 8, 9, 10,11,12,13,14].

## 2. Laser Driven Acceleration

Electron plasma waves (EPW) provide the basic conditions for the generation of accelerating electric fields in plasmas. Several schemes can be employed to excite EPW in plasmas. A simple approach is based upon intense laser pulses to induce strong perturbations in the electron density distribution. Initially, the so-called laser beat-wave technique was adopted (see [15] and references therein) to produce sufficiently strong electron density perturbations and the subsequent formation of relativistic electron plasma waves.

More recently, with the advent of CPA technique, a single, very intense laser beam can be focused inside a plasma to generate an EPW along the laser propagation path, leading to a substantial reduction of the complexity of the

experimental set up. If the longitudinal size of the laser pulse is about half (or less) of the wavelength of the natural oscillation mode ( $\lambda_p$ ) of the plasma, a high amplitude plasma wave develops quasi-resonantly on the wake of the pulse, excited by the action of the longitudinal ponderomotive force [16]. Since  $\lambda_p$  depends on the plasma density ( $n_e$ ) through the plasma frequency ( $\omega_p$ ):

$$\lambda_p = \frac{2\pi c}{\omega_p} \propto \frac{1}{\sqrt{n_e}}$$

the condition for the quasi-resonant growth can be expressed as follows:

$$\tau_{laser} c \approx \frac{\lambda_p}{2} \Leftrightarrow \tau_{laser} \approx \frac{T_p}{2} \Leftrightarrow n(cm^{-3}) \approx \frac{3 \cdot 10^{-9}}{\tau_{laser}^2(s)}$$

where  $\tau_{laser}$  and  $T_p$  are the laser pulse duration and the period of the electromagnetic field respectively. The detailed description of the EPW excitation and evolution, along with the dynamics of the laser pulse inside the plasma, can be achieved by means of fully relativistic particle codes.

The Laser Wake-Field Acceleration (LWFA) is considered a quasi-resonant process, in the sense that the resonant condition is not so severe. The crucial issue here is the identification of key experimental parameters that allow a significant control of the interaction conditions required to ensure reproducibility of acceleration performance. In the following we identify two schemes in which the aspects of quality and control are faced with different approaches.

## 2.1. Electron acceleration in EPW by self-trapping

In this case the energy gain of the electrons depends on the conditions of the injection in the EPW (i.e. electron velocity and phase of the wave) and those of their expulsion from the wave. This scheme has been widely studied experimentally and electron energies above 100 MeV level have been achieved and reproduced in a number of laboratories world-wide.

In a recent experiment [17] performed at the Laboratoire d'Optique Appliquée, very collimated bunches of high energy electrons have been produced by focusing a super-intense femtosecond laser pulse in sub-millimetre under-dense plasmas. The density of the plasma, pre-formed with the laser exploding-foil technique, was mapped using Nomarski plasma interferometry. The electron

beam was fully characterised: up to  $10^9$  electrons per shot were accelerated, most of which in a beam of aperture below  $10^{-3}$  sterad, with energies up to 40 MeV. These measurements, which are well modelled by 3-D numerical simulations, validate a reliable method to generate ultra-short and ultra-collimated electron bunches. Fig.1 shows a typical radiochromic film result [18] after a single exposure to the electron beam generated by focusing the CPA pulse at an intensity of  $\approx 8 \times 10^{19} \text{ W/cm}^2$  in the plasma produced by the explosion of a  $1 \mu\text{m}$  thick target. These images show a small central spot very closely aligned with the laser propagation axis. This feature is visible on all the seven layers while other features surrounding this bright spot are only visible on the first layer. These results suggest that besides an intense electron flux of lower energy in a ring of  $\theta_{\text{ring}} \approx 18$  deg aperture, there is a bunch of very collimated, high energy electrons accelerated along the laser propagation axis,  $\theta_{\text{bunch}} < 1$  deg.

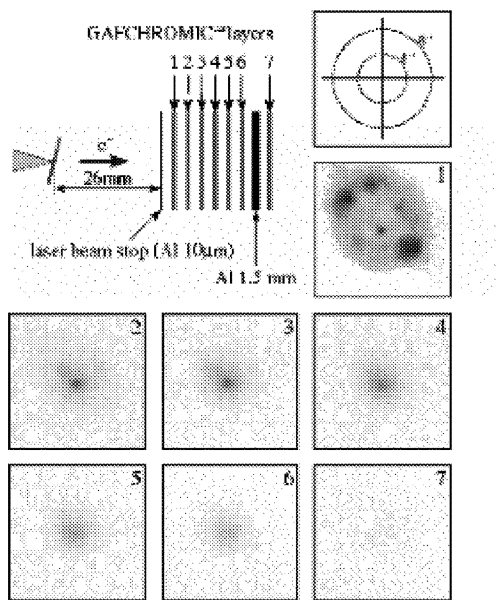


Figure 1. Densitometer scans of the radiochromic films (see insert) after exposure to the energetic electron beam produced by interaction of an ultraintense laser pulse with a preformed plasma located at 26 mm from the first film. The CPA pulse intensity in the plasma is  $8 \times 10^{19} \text{ W/cm}^2$ . The angular scale is also shown for reference.

The experimental results have been compared with the predictions of numerical simulations carried out using a three-dimensional particle-in-cell code with a plasma density profile and a laser pulse intensity distribution very close to the experimental ones. The angular distribution obtained from the simulations

clearly shows the main feature of that observed experimentally, namely the central, collimated electron beam is well reproduced. A typical spectrum of the accelerated electrons is shown in Fig.2 (black dots). According to this plot, the electron beam consists of a sizeable number of electrons with energies from a few MeVs up to 40 MeV. Also plotted in Fig.2 (solid line) is the calculated spectrum of the very collimated, high energy electrons accelerated along the laser propagation axis, obtained from the PIC simulation. There is a very good agreement between the experimental spectrum of the high energy electron beam and the simulated one.

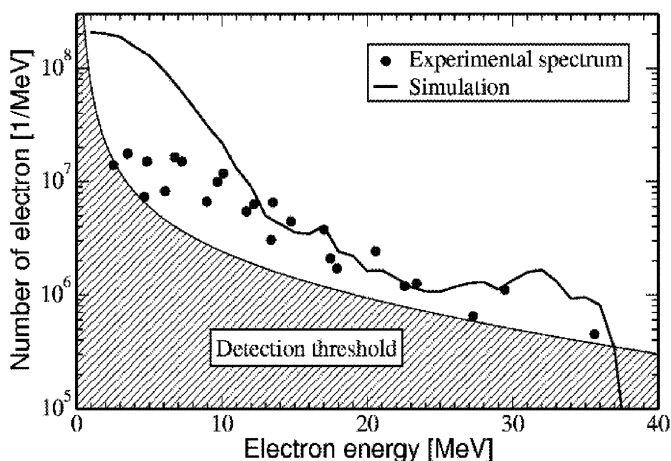


Figure 2. Spectrum of the electrons in the collimated beam. Filled circles represent the experimental electron spectrum. Also shown is the detection threshold of the electron spectrometer. The solid line is the spectrum of the electrons in the collimated beam as obtained from the PIC simulation.

The kind of target used to produce the plasma in which the electric field of the Langmuir waves can accelerate the electrons is one of the main point to be addressed in the experiments. In fact the conditions for an effective and controlled acceleration concern the laser parameters (intensity, pulse duration, focal spot diameter, pulse/pre-pulse contrast ratio,...) as well as the plasma parameters (dimensions, density distribution, temperature,...). Gas jets are now regarded as the most promising targets because they allow high repetition rate for the laser-target interactions and satisfactory control of the electron density distribution of the produced plasma [19, 20].

In a recent experiment at SLIC facility (CEA-Saclay) the interaction of 60fs laser pulses with gas jet targets has been studied by using optical diagnostics and detectors for energetic particles and X/ $\gamma$  radiation. The maximum laser intensity was, in the focal spot,  $10^{19} \text{Wcm}^{-2}$ . In this regime of fairly relativistic

laser intensities, different experimental parameters have been varied to match the best conditions for the production of energetic electron bunches.

The experiment was performed with a 10 TW Ti:Sa laser system operating in the CPA mode and delivering up to 0.6 J in 60-fs pulses at 800-nm. The contrast of the main laser pulse on both the nanosecond and picosecond scale were measured by a third order auto-correlator. The nanosecond contrast, due to Amplified Spontaneous Emission (ASE), was found to start about 1ns before the main pulse with a contrast ratio of  $\approx 10^{-6}$ , while the *pedestal* of the femtosecond pulse, due to the pulse compression, had a contrast ratio of  $\approx 10^{-4}$  for a duration of about 1ps before the main pulse. These values are typical of most high power femtosecond lasers.

The pulse was focused in the gas jet using a 200 mm, silver coated off-axis parabolic mirror. The numerical aperture of the focusing optics was f/2.5 and the maximum focused nominal intensity was  $10^{19} \text{ Wcm}^{-2}$  in a slightly elliptical focal spot whose horizontal and vertical diameters were 8 $\mu\text{m}$  and 10 $\mu\text{m}$  FWHM respectively. The corresponding normalised field parameter in the focal spot was  $a_0 = 2.2$ . A fraction of the main femtosecond pulse was frequency-doubled using a 2 mm thick, type I KDP (Potassium Dihydrogen Phosphate) crystal and used as an optical probe propagating perpendicular to the main pulse, in a Mach-Zehnder interferometer configuration. The probe pulse is expected to have a pulse duration of approximately 120 fs, due to group velocity dispersion in the 2mm frequency doubling crystal. The gas-jet was delivered by a 1 mm diameter, cylindrical nozzle. The maximum gas pressure in the valve was about 8 bar corresponding to a neutral gas density in the jet greater than  $10^{19} \text{ atoms/cm}^3$ . The value of neutral gas density as well as the plasma density was obtained from a Fourier analysis [21] of the fringe pattern taken with the Mach-Zehnder interferometer.

A systematic study of the energetic electron production has been performed for different plasma densities (changing gas type (He, N<sub>2</sub>) and pressures), plasma shapes (changing the nozzle) and for different focusing points with respect to the gas jet (see Fig.3).

The major production of energetic electrons has been observed when the main laser pulse was focused at the border of the gas plume (right side in the Fig.3) and for the highest plasma densities attained with the employed apparatus (N<sub>2</sub> pressure in the valve at about 8 bar). Moreover the production of energetic electrons was rather unpredictable, even if clearly correlated with the enhanced propagation of the fs laser pulse, most likely due to the on set of the beam self-focusing.

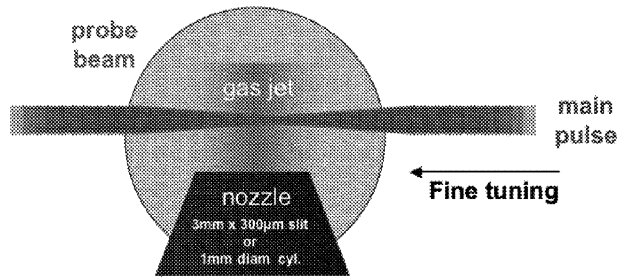


Figure 3. Detail of the gas jet and the interaction region.

To get a quantitative information about the energy spectrum of the produced electrons a plot of the released energy as a function of the incident electron energy is calculated for each layer of the detector by means of MonteCarlo simulations.

The measured dose (obtained by scanning the radiochromic films) is then converted into electron energy distribution. In Figure 4 the number of electrons produced per MeV as a function of their energy in MeV are plotted for four shots to evidence the variability of the acceleration process. As one can see in some shots energetic electrons up to 3 MeV have been produced.

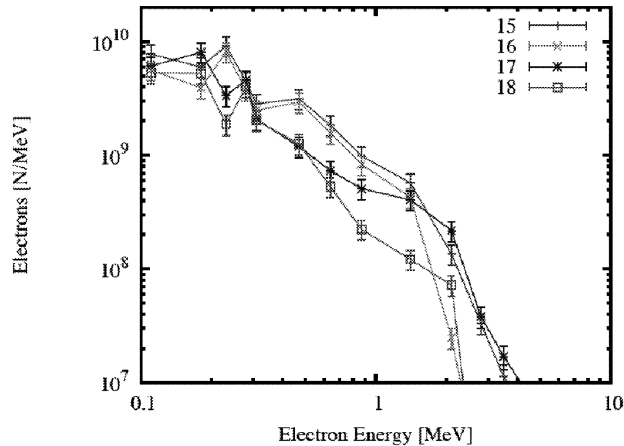


Figure 4. Electron energy distribution at 7.6 bar N<sub>2</sub> pressure in the gas valve.

From the space distribution of the dose on the first radiochromic film, that was 7mm apart from the laser produced plasma, come out the electrons were emitted forward in a cone of about 60° full aperture.



## 2.2. Suitably shaped pre-formed plasma

Several teams are investigating, by theoretical and experimental approaches, different possibilities of reducing the energy spread of the electrons accelerated by laser plasma techniques.

In 1998 S.Bulanov et al [22] proposed a novel scheme for the production of high-quality electron beams in LWFA in which a controlled longitudinal non-linear wave-breaking is induced by an electron density depletion. This proposal was supported by both analytical and numerical results in a one dimension configuration. In fact, if the plasma density decreases in the direction of the pulse propagation (z coordinate), the wave number k increases with time and the very simple relation holds:

$$\frac{\partial k_p}{\partial t} = -\frac{\partial \omega_p}{\partial z}$$

The resulting decrease of the phase velocity, at the interface between two uniform density regions, makes the wave to break, even when its initial amplitude is below the wave-breaking threshold. As a result of the break at the interface between the two regions, fast electrons from the wave crest are trapped by the wave and are pre-accelerated into the lower density region where the wake field remains regular. An energy balance argument shows that in the weakly inhomogeneous case the relative density of fast electrons is approximately given by the ratio

$$\frac{v_{ph}}{\omega_{pe} L}$$

where  $\omega_{pe}$  is the plasma frequency at the interface and L its inhomogeneity length. In the following the results of PIC simulations concerning such an acceleration scheme will be shortly presented [23]. In Fig.5 the electron density map of a pre-formed plasma, consisting of two quasi uniform regions with a sharp transition, is reported. After a smooth vacuum-plasma transition, the longitudinal profile of the electron density reaches a first plateau ( $n_e=2.1 \cdot 10^{19} \text{cm}^{-3}$ ) and then it decreases abruptly with a scale length  $L=2\mu\text{m}$  to a second plateau ( $n_e=1.1 \cdot 10^{19} \text{cm}^{-3}$ ). In the same figure the electron plasma wave excited by a laser pulse propagating in the plasma is apparent, as well as the first bunch of accelerated electrons (see the arrow).

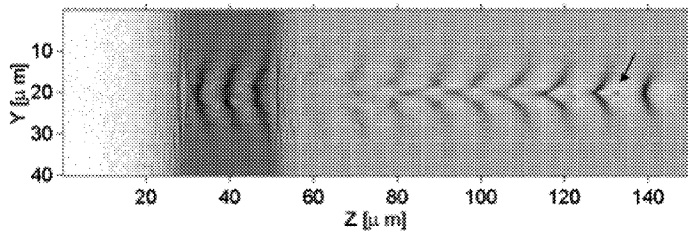


Figure 5. Electron density map of the pre-formed plasma, with a sharp density depletion, crossed by an intense laser pulse: 17fs,  $\lambda=1\mu\text{m}$ ,  $I=2.5 \cdot 10^{18}\text{W/cm}^2$ . The excited electron plasma wave as well as the accelerated electron bunch (arrow) is apparent.

The energy spectrum of the accelerated electrons is reported in Fig.6. We can see that, selecting the electrons with energy exceeding 7MeV, the resulting bunch of  $N_e \approx 10^8$  electrons with energy  $E \approx 10\text{MeV}$  is characterized by a remarkable good quality and has an energy spread  $\Delta E/E \approx 5\%$ , transverse and longitudinal size  $\delta y \approx 1\mu\text{m}$ ,  $\delta z \approx 5\mu\text{m}$  respectively and emittances

$$\mathcal{E}_{rms}^r = 9 \cdot 10^{-2} \text{mm} \cdot \text{mrad} \quad \mathcal{E}_{rms}^{lon} = 2 \text{mm} \cdot \text{KeV}.$$

The possible applications of such high quality beams include injection of electrons in a LINAC accelerator for the production of high energy beams and the production of ultra-short pulses of X rays with linear and non linear Thomson backscattering.

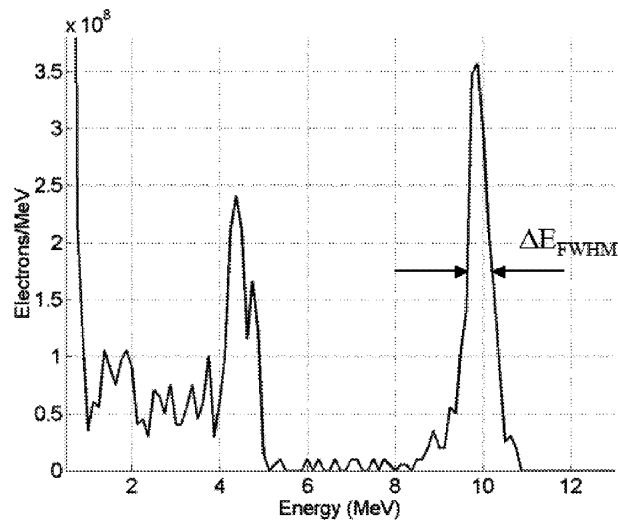


Figure 6. Energy spectrum of the accelerated electrons in pre-formed plasma with a sharp density depletion.

### 2.3. Acceleration of externally injected electrons

The idea here is to inject electron bunches produced by an external source in the electron plasma wave in such a way that the electrons experience a huge accelerating field and their energy is thus increased in a very short distance. In this configuration, the external source of electron bunches can be either a conventional photo-injector or a plasma photo-injector as described in previous sections.

As in the case of self-injection, also external injection was initially pursued using the so-called laser beat-wave driven relativistic plasma wave. However, experiments carried out so far using intense, ultrashort CPA pulses have demonstrated acceleration gradients which are up to two orders of magnitude larger than those achieved in laser beat-wave experiments and suggest a perspective of much more compact accelerators [24], provided that schemes for relatively long interaction length are demonstrated.

The injection of monochromatic electron bunches from a LINAC into plasma waves, previously excited by a super-intense and ultra-short laser pulse propagating in a pre-formed plasma, is one of most ambitious goals of three sub-disciplines: accelerator physics, plasma physics and laser physics. This acceleration scheme can allow, in principle, high energy and monochromatic electron bunches to be produced in a very short distance. However severe constraints have to be fulfilled to get the required low values of emittance and energy spread. In fact the electron bunch length have to be much shorter than the plasma wave wavelength and the injection phase has to be controlled within a few degrees of the plasma oscillation. For instance in the case of a plasma wavelength of 200-300  $\mu\text{m}$ , the electron bunches have to be shorter than 10  $\mu\text{m}$  and synchronized with the laser pulse within less than 100fs.

Here we describe the result of a numerical simulation in which an electron bunch produced by a LINAC, at a given energy, is injected into a plasma for further acceleration. The simulation technique is based upon a test-particle code that assumes a quasi-static field approximation. Transverse fields are neglected, while non-linear effects are treated in a 2-dimensional representation. The injected electron bunch has a charge of 21 pC at an energy of 130 MeV, in an 8  $\mu\text{m}$  transverse size and a longitudinal size of 12  $\mu\text{m}$ . The energy spread is assumed to be 0.1%.

From the point of view of the laser-plasma accelerator, the simulation uses a 4J, 100 fs duration pulse at 800 nm wavelength, focused in a 50  $\mu\text{m}$  focal spot. This laser pulse is focused in a preformed plasma at a density of  $1.5 \times 10^{17} \text{ cm}^{-3}$ . The maps of Figure 7 show the electron density distribution of the electron plasma wave excited by the laser and the associated longitudinal electric field.

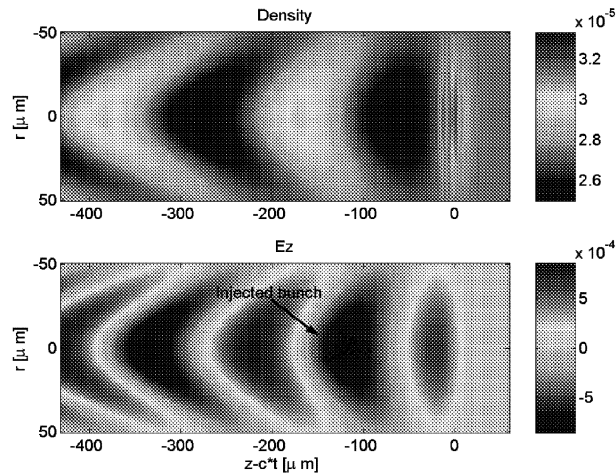


Figure 7. (top) Map of the electron density, normalized to the critical density at 800 nm, showing the charge separation of the electron plasma wave induced by the high intensity laser pulse. (bottom) Map of the longitudinal electric field associated to the EPW. Also visible in the frame is the bunch of externally injected electrons.

The bunch, also visible in the map, has a longitudinal extent which is small compared to the wavelength of the EPW. The energy distribution of the electrons at the exit of the plasma is shown in Figure 8 for two different plasma acceleration lengths of 20 mm and 100 mm.

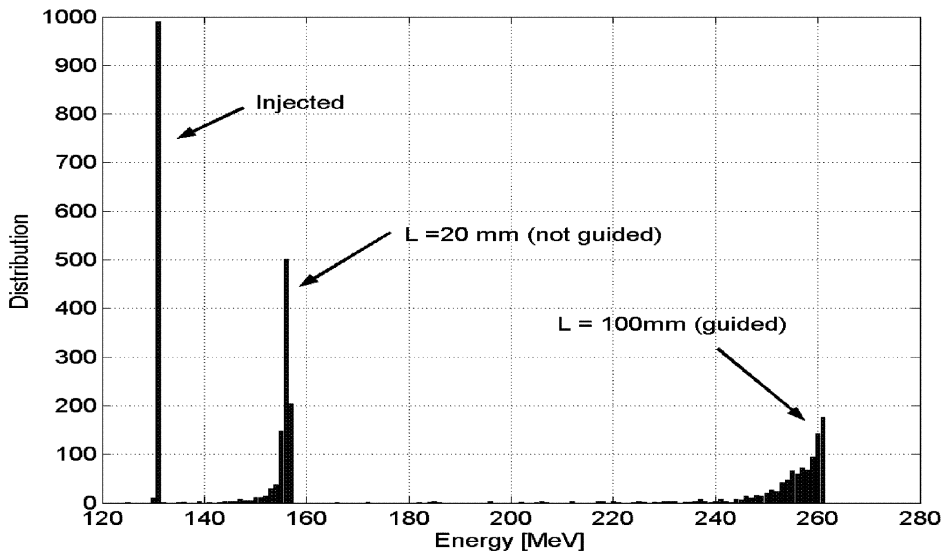


Figure 8. Electron energy distribution at the exit of a plasma of  $1.5 \times 10^{17} \text{ cm}^{-3}$ , for an acceleration length of 20 mm, corresponding to twice the Rayleigh length  $Z_R$  of the focusing optics. Also shown in the plot is the result of an accelerator length of 100 mm, assuming a laser pulse guiding over  $5 Z_R$ . The energy spread of the output electrons is 3% (rms).

These results provide us with a well defined range of parameters that are the ground on which the performance of the laser facility proposed in the PLASMONX project will operate (see section 4.). Together with the calculation tools benchmarked with test experiments carried out so far, they supply a powerful and robust framework for the R&D activity on laser-driven acceleration at LNF.

### 3. Laser Produced Proton Beams

When an ultra-intense laser pulse is focused on a solid target a sizeable fraction of the laser energy is transferred to charged particles [25]. In particular, the generation of multi-MeV proton beams has been observed. Such proton beams are now under consideration for application in radiotherapy as well as medical diagnostic. In spite of the growing interest on laser produced proton beams, the physical mechanisms of generation and acceleration of such protons is only partially understood, even if it undoubtedly concerns the electric field produced by the fast electron escaping the irradiated target.

During an experimental campaign at CLF, the Vulcan Nd:glass laser operating in the Chirped Pulse Amplification mode was used to investigate this mechanism. The targets used for the production of the proton beams were 1 mm wide and about 1 cm long Al foils. The target thickness was 25, 100 or 250  $\mu\text{m}$ . The energy of the laser pulse was about 100 J. The diameter of the focal spot on target was about 10  $\mu\text{m}$  (FWHM) containing almost 40% of the energy. The duration of pulse was 1 ps allowing intensities up to  $10^{19} \text{ Wcm}^{-2}$ . The protons were detected using several layers of Radio-Chromic Films (RCF). A schematic experimental setup is shown in Figure 9.

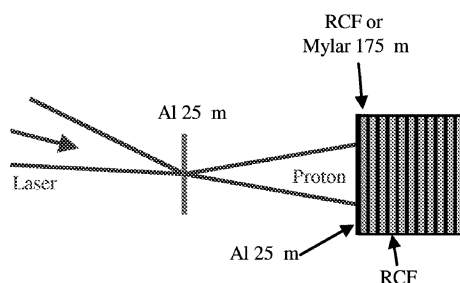


Figure 9. Experimental setup for the detection and characterization of proton beams.

A fundamental step towards the experimental characterization of laser produced proton beams is the use of a detection technique capable of providing good spatial and spectral resolution in single shot measurements and in the presence of the large electromagnetic noise typical of high power, ultrashort laser interaction experiments.

The detection technique based on RCF exploits the proportionality between the optical density (OD) variation of active layers and the energy deposited locally by the impinging particle beam (absorbed dose). The main disadvantage in the use of RCF is that from the signal recorded it is not possible to discriminate between different types of ionizing particles (electrons, protons or other kind of ions). Therefore additional measurements, possibly based upon track particle detectors (e.g. CR39) are used to identify the nature of particles.

A straightforward interpretation of data from RCF does not provide immediately a complete spectral information. A numerical analysis is required in order to reconstruct the proton beam spectrum. An algorithm was developed [26,27] to reconstruct the energy-dependent proton density. The main idea behind the algorithm is to reconstruct the proton angular distribution and spectrum at a particular sampling energy. The choice of this energy value is obtained by comparison with the response of the detector to monochromatic and mono-directional protons beams. The numerical expression of the detector response is calculated by means of a Montecarlo simulation.

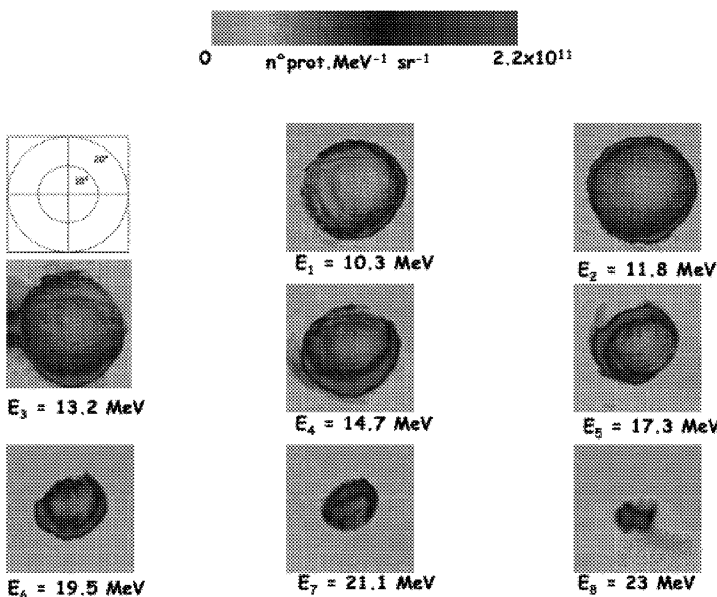


Figure 10. Angular distribution at different proton energies.

Let us consider data from a typical shot taken in the case the target was a 25  $\mu\text{m}$  thick Al foils. The generated proton beam was detected using a stack of RCF type MD-55 by Gafchromic. The numerical reconstruction of the proton beam profile is reported in Figure 10 where the angular distribution of the protons at the sampling energies for both shots are shown. The space resolved spectrum shows a ring where the proton density is enhanced, with a decreasing radius for increasing proton energy, as previously observed with CR39 detectors [28]. This is a clear evidence that protons are emitted with a quasi-monochromatic component localized at the center of the beam.

#### 4. PLASMONX

The aim of the PLASMONX (**PLAS**ma acceleration and **MON**ochromatic **X**-ray production) project is to provide LNF with a world-class, high-power laser facility suitable for the development of an innovative, high-gradient acceleration technique based upon super-intense and ultra-short laser pulses, and X/ $\gamma$ -ray tunable sources, using Thomson scattering of optical photons by energetic electrons. The facility will be built in close interaction with the SPARC project [29] presently in progress at LNF. The main purpose of the facility will consist in R&D activity aimed at the following objectives:

demonstration of high-gradient acceleration of electrons injected into electron plasma waves excited by ultra-short, high power laser pulses;

development of a monochromatic and tunable X-ray source in the 20-1000 keV range, based upon Thomson Scattering of laser pulses by relativistic electrons.

Both lines require very bright and short electron bursts together with very high power laser pulses of sub-100fs duration. Studies at the forefront of research in this field consistently indicate that the power level and the focused intensity for a laser system appropriate for these studies are  $>10$  TW and  $>10^{19}\text{W}/\text{cm}^2$  respectively.

An important point to face in this kind of experiments concerns the design of the target on which the super-intense laser pulse is focused. In fact while plasmas produced from gas jet targets are very suitable for electron acceleration, thin foils are been fruitfully experimented in high energy proton/ion production.

The R&D activity carried out at this facility will be open to some extent to external users, in particular for what concerns bio-medical oriented uses [30] of the available sources for diagnosis and therapy.

## 5. Conclusions

Laser-driven acceleration is now emerging worldwide as a mature approach to particle acceleration. The paper reports on recent results obtained in the major European facilities involved in this field. The idea of embedding a highly advanced laser laboratory in a LINAC dedicated laboratory is a necessary step in order to establish this technology in Italy. With the ongoing SPARC activity dedicated to FEL development at LNF, the PLASMONX initiative is most appropriate and timely. Chances of success of the proposed program and the possibility of achieving high impact scientific results in the field of compact accelerators and ultra-short X-ray sources are now very high and call for a prompt transition from planning to execution.

## Acknowledgments

We would like to thank the staff of the LOA, CLF-RAL and SLIC facilities for their invaluable and friendly support. We also acknowledge the LASERLAB EUROPE Trans-national Access Programme and the CINECA High Performance Computing.

## References

- 1 Tajima T. and Dawson J.M., *Phys.Rev. Lett.*, **43**, 267. (1979).
- 2 Strickland D. and Mourou G., *Opt. Comm.*, **56**, 219.(1985).
- 3 Katsouleas T., *Nature*, **431**, 515 (2004).
- 4 S.P.D. Mangles et al., *Nature*, **431**, 535 (2004).
- 5 C.G.R. Geddes et al., *Nature*, **431**, 538 (2004).
- 6 J. Faure et al., *Nature*, **431**, 541 (2004).
- 7 V. Malka et al., *Laser and Particle Beams*, **20**, 217-221 (2004).
- 8 H. Hora et al., *Laser and Particle Beams*, **18**, 135-144 (2000).
- 9 K. Nakajima, *Laser and Particle Beams*, **18**, 519-528 (2000).
- 10 F. Dorchies et al., *Laser and Particle Beams*, **17**, 299-305 (1999).
- 11 K. Nakajima, *Laser and Particle Beams*, **18**, 519-528 (2000).
- 12 F. Dorchies et al., *Laser and Particle Beams*, **17**, 299-305 (1999).
- 13 S.V. Bulanov, V.S. Khoroshkov, *Plasma Phys. Rep.* **28**, 453, (2002).
- 14 M. Borghesi et al, *Phys. Rev. Lett.*, **88**, 135002, (2002).
- 15 C. Joshi et al., *Nature*, **311**, 525 (1984).
- 16 E. Esarey et al., *IEEE Trans. On Plasma Sci.* **24** (2) 252 (1996).



- 17 D. Giulietti et al., *Phys. Plasmas*, **9**, 3655 (2002).
- 18 M. Galimberti et al., *Rev. Sci. Instrum.* **76**, 053303 (2005)
- 19 J. Faure, V. Malka, J.-R. Marques, et al., *Phys. Plasmas* **10**, 2039, (2003)
- 20 C.B. Schroeder, E. Esarey, C.G.R. Geddes et al., *Phys. Plasmas* **7**, 3009, (2000)
- 21 M. Takeda, H. Iwano, and S. Kobayashi, *J. Opt. Soc. Am.* **72**, 156, (1982); K.A. Nugent, *Appl. Opt.* **18**, 3101 (1985).
- 22 Bulanov S. et al., *Phys. Rev.E*, 1998
- 23 Tomassini P. et al, *Phy. Rev. Special Topics-A&B*, **6**, 121301, 2003
- 24 F. Dorchies et al., *Phys. Plasmas* **6**, 2903 (1999).
- 25 S.J. Gitomer et al., *Phys. Fluids*, **29**, p. 2679 (1986)
- 26 E. Breschi et al., *Nuclear Instr. and Methods A*, **522**, p. 190 (2004)
- 27 E. Breschi et al., *Laser and Part. Beams*, **22**, p. 393 (2004)
- 28 E. Clark *et al*, *Phys. Rev. Lett.*, **84**, p. 670 (2000)
- 29 D. Alesini et al., *NIM-A* **507** (2003) 345-349.
- 30 D. Giulietti, The Congress of Società Italiana di Fisica, Brescia, 2004.